Reviewer 2:

Thank you for your questions. In the following, the reviewer's comments are italicized.

RC2: *(1) The stability associated with the SL method is that the deformational Courant number (Lipschitz condition) should not exceed unity, in plain language, the trajectories should not cross intersect (see, Staniforth & Cotes 1992 MWR paper). Is the cubic ISL method (lines 115-120) unstable due to this condition? Need some explanation.*

No. In the first example, lines 118–122, the flow is uniform in space and constant in time. Thus, the trajectories are parallel lines and so cannot intersect. In addition, the deformational Courant number is 0 because the flow is uniform in space.

The second example, described in lines 123–127, is more complicated. We analyze this case in Appendix A of this letter.

RC2: *(2) The SL transport scheme can be stabilized using a limiter, filter or with an explicit diffusion (see, Ullrich & Norman, QJRMS, 2014). You can use the native high-order SE interpolation (basis function) for the SL transport combined with the limiter which you are already using for the Islet method. It will be interesting to see how the Islet method compares with this simple SL-SE scheme employing 4x4 GLL grid (I guess that is the SE grid choice made for the operational E3SM).*

A limiter or filter makes a linear discretization nonlinear. A method that assures boundedness of the solution leads to stability because the solution is bounded in norm. However, for a nonlinear discretization, consistency and stability are not enough to assure convergence. In contrast, our method satisfies a necessary condition for stability of a linear discretization; because the discretization is linear, consistency and stability assure convergence.

The dash-dotted curves in Figure 6 of the manuscript illustrate what happens when "*the native high-order SE interpolation (basis function) for the SL transport [is] combined with the limiter*." The curves for $n_p^{\mathrm{t}} > 4$ diverge within one cycle of the test problem. The $n_p^{\mathrm{t}} = 4$ case only starts to diverge, but with multiple cycles or greater refinement, the divergence continues to be as substantial as in the $n_p^{\mathrm{t}} > 4$ cases. This divergence is a result of the fact that the linear discretization's maximum eigenvalue magnitude is above 1 at almost every value of Δt, as illustrated by the red curve in Figure 2 of the manuscript for the case $n_p = 8$.

We discuss the reference Ullrich & Norman, 2014 [6], in Appendix B of this letter.

RC2: *(3) It is not convincing to have 3 grid systems (physics: FV, dynamics: GLL, transport: tweaked GLL) in a SE modeling framework. The Fig.5 shows such a grid configuration, and it appears to be very challenging. At a very high (NH) resolution the data movement is a major issue for an element-based Galerkin model (DG/SE). A typical climate model may have O(100) tracers, an additional tracer grid with more DOF than the dynamic grid can exacerbate this problem. This will limit the use of Islet scheme, how do you address it?*

The Energy Exascale Earth System Model version 2 (E3SMv2) uses a two-grid system as a result of work described in [1]. Semi-Lagrangian transport, with $n_p^{\mathrm{v}} = n_p^{\mathrm{t}} = 4$, and this two-grid system, with $n_f = 2$, together make the E3SMv2 Atmosphere model twice as fast as E3SMv1. Figure 1 shows a representative strong-scaling study comparing version 2 to version 1. I believe the success of this two-grid system motivates further work along these lines.

Regarding many tracers, in the case of $n_p^{\mathrm{t}} = n_p^{\mathrm{v}} = 4$, Figure 27 of the manuscript is illustrative. This figure shows dynamical core performance for the full 3D method on a 3.25km cubed-sphere grid having 128 model levels. The throughput of the dynamical core with SL transport is only slightly decreased when going from 10 tracers to 40 (1.38 to 1.24 SYPD on 27,600 Summit V100 GPUs), while the throughput of the dynamical core with Eulerian transport is decreased substantially (0.97 to 0.44 SYPD with the same number of GPUs). Section 4.3 of the manuscript discusses

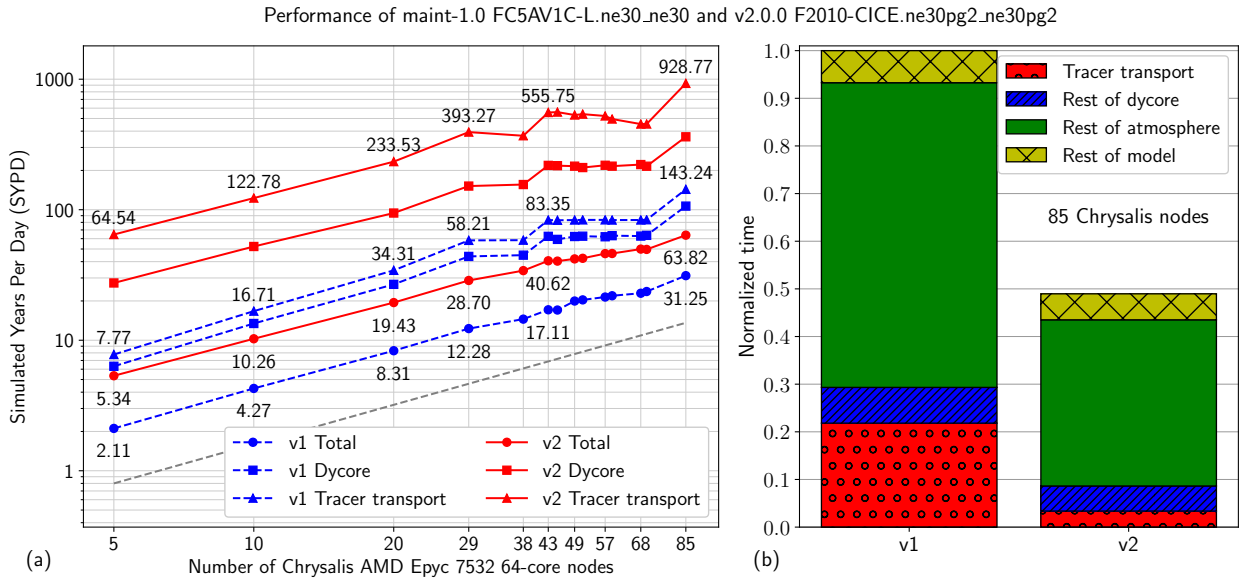

Figure 1: Performance of the Energy Exascale Earth System Model (E3SM) version 2 Atmosphere Model (EAMv2) on the ANL LCRC Chrysalis cluster. (a) Strong-scaling study of the standard-resolution version 1 (v1, blue) and version 2 (v2, red) models. Each model has 40 tracers. Tracer transport is over 6 to over 8 times faster than in v1 due to use of semi-Lagrangian transport in v2. The overall model ("Total") is 2 to 2.5 times faster than v1, with most of the remaining speedup due to the use of separate physics parameterizations and dynamics grids. (b) Proportion of time spent in key subcomponents, with the total v1 time normalized to 1, for the models run on 85 Chrysalis nodes. Tracer transport, red with circles, is sped up by almost 6.5. The green region encapsulates the part of the model that uses the physics grid; it is decreased by a factor 1.8 in v2.

the communication details for $n_p^{\mathrm{t}} > n_p^{\mathrm{v}}$. Importantly, only the fundamental step of the method, obtaining interpolated values, scales in communication volume proportionally to $(n_p^{\mathrm{t}})^2$; a scaling of this sort is true of any method as basis order increases. Equally importantly, there are no additional communication rounds when $n_p^{\mathrm{t}} > n_p^{\mathrm{v}}$.

RC2: *(4) With real data you have velocity information only available at the GLL (dynamics) grid, the way you find the 2D trajectory information using the 3D Cartesian coordinates leads to additional computational overhead when the method is extended to the 3D application (line 470-475). This needs some justification, why not use the spherical (u,v) components or corresponding contravariant vectors?*

Figure 27 of the manuscript shows results for the full 3D application, and Figure 1 of this letter also uses the full 3D solver. (u, v) should not be used because of the poles. Contravariant components can be used but require details to handle coordinate systems between elements. Cartesian coordinates avoid these details at the cost of one extra variable. However, the trajectory computation is a negligible part of the overall transport step even at just 10 tracers, making this extra variable also negligible. Finally, as either or both of n_p^{t} and tracer count increase, the relative cost of the trajectory computation decreases.

RC2: *It is not clear that the maximum eigenvalue required for the interpolation is the tracer data dependent, in that case you have a serious computational overhead for the multi-tracer applications, Please clarify!*

The maximum eigenvalue computation is used only in deriving basis sets. It is not used in a simulation. I am sorry that this point was not clear in the manuscript.

RC2: *What is the computational halo requirement for an SE stencil with NxN GLL points, when the shape preserving limiter is applied?*

The limiter requires extrema data from adjacent elements. The extrema data per adjacent element is two scalars, independent of n_p^t. Thus, the relative cost decreases with increasing n_p^t. This communication pattern is the same as for the original Eulerian SE method used in the SE dynamical core.

RC2: *(5) What is the special advantage of using Islet method? It seems you have introduced a complex numerical method for a relatively simple linear transport problem.*

Although the transport problem may be simple, it can have a large computational cost in Earth system models because of the large number of tracers. Thus, this work focuses on improving computational efficiency, like other projects that develop tracer transport methods for passive tracers, e.g., those in [3]. Computational efficiency is the ratio of a measure of solution accuracy to a measure of computational work. The Islet method combines a very efficient class of SL methods, the remap-form interpolation class, with details specific to element-based methods. It provides two parameters, n_p^t and n_f, to efficiently trade between accuracy and speed. Importantly, it does not require the dynamics solver to be modified, regardless of parameter values, making it possible to tune tracer transport parameters without also having to modify the dynamics solver.

Similar reasons led to the work to separate the physics and dynamics grid [2, 1]. In both these papers, additional complexity was introduced to transfer data between grids. But the result was an increase in computational efficiency in each Earth system model.

RC2: *If mass-fixing is the way to go, one could use the RBF-based (Kriging type) interpolator which provides very accurate solution, and no need for the expensive search for max eigenvalue etc.*

Interpolation methods require careful stability analysis. This is in contrast to exactly integrated L^2 projection methods, in which the projection provides stability. Interpolation methods can be substantially more efficient than projection methods, justifying the effort to do this analysis and to derive methods satisfying linear stability conditions. Because the Islet bases provide element-local interpolation, the stability analysis can focus on the element. An interpolation method that uses data beyond a single element would require mesh-dependent stability analysis. Its implementation would require greater communication volume than an element-local method. An RBF-based method may be effective, but work would need to be done to analyze and implement it. The manuscript focuses on an element-local interpolation basis.

Regarding the "expensive search for max eigenvalue," I am sorry that it was not clear in the manuscript that this search is done only to find basis functions. Once the basis function sets are found based on analysis of an element, e.g. those in Table 1, they can then be used directly in simulations like any other basis function set.

Thanks,
Andrew Bradley

Appendix A

By equation A6 of [5], two computed trajectories, which are line segments, intersect when there is a point in space-time at which these computed trajectories have the same position. A bound of one on deformational Courant number is a sufficient condition to assure that these computed trajectories do not cross when they are computed according to certain algorithms. In addition, the deformational Courant number is used in, e.g., [5, 4] to bound the time step when solving iteratively for the departure points. In the examples I provide in section 2.1, trajectories are exact, and thus no condition governing the solution of the departure point is needed. Importantly, given exact trajectories, the deformational Courant number is not a means to assess stability of the space-time operator, as demonstrated in the first example.

In the second example, the flow is shear and constant in time. The deformational Courant number is $\max_{x,y} \max(|u_x|, |u_y|, |v_x|, |v_y|)\Delta t = 2\pi\Delta t$; thus, with $\Delta t = 0.2761$, the number exceeds 1. However, trajectories in this flow cannot cross, in two senses, as follows. First, the exact trajectories do not cross. Second, line segments connecting arrival points to exact departure points do not cross. The second follows from the first, which we shall demonstrate in a moment, because the exact trajectories in this flow are lines. For in this flow, (i) velocities are constant along lines, (ii) a velocity vector points along its constant-velocity line, and (iii) these lines of constant velocity are parallel to each other. Consider any two points in the flow and a time increment Δt. By (ii) a point must stay on the line on which it started. By (i) a point on a line cannot overtake another point on that line. Finally, by (iii), if the two points start on separate lines, since their lines do not cross, the trajectories cannot, either. For this flow, we should also verify that each departure element is neither self-intersecting nor has reversed in orientation, both of which are possible in a discretization even if the continuum flow does not permit intersecting trajectories. I verified using orientation and convexity checks, where the latter is a sufficient condition for non-intersection, that no deformed element has reversed orientation or is self-intersecting. Finally, whereas the time step 0.2761 in this example leads to an unstable operator, time steps 0.273 and 0.279 do not.

Between the two examples, we see that a unit bound on the deformational Courant number, given exact trajectories and so exact departure points, is neither a necessary nor a sufficient condition for stability of the space-time operator. Similarly, the violation of the bound is neither a necessary nor a sufficient condition for instability.

Appendix B

Ullrich and Norman present a scheme that is third-order accurate when a monotonicity scheme is not applied, requires hyperdiffusion for stability in 2D, and is CFL-limited by hyperdiffusion [6]. The left panel of Figure 11 of [6] suggests that if a positivity filter is applied, the method has an empirical order of accuracy of approximately 2.5. Positivity—the tracer must have values at least 0—is a weaker condition than monotonicity, which requires that a tracer value in a region R is bounded below and above by values in the domain of dependence of the region R, where the definition of R depends on the discretization. In the manuscript, results for the Islet method are shown with a monotone filter rather than just a positivity filter. Hyperdiffusion requires additional communication rounds. As the basis order increases, the hyperdiffusion-limited CFL number roughly decreases, from 2.44 for cubic to below 1 for quintic. Islet does not require a filter or hyperdiffusion for stability, regardless of basis order, and we find bases providing order of accuracy up to 9.

References

[1] W. M. Hannah, A. M. Bradley, O. Guba, Tang Q., J.-C. Golaz, and W. Wolfe. Separating physics and dynamics grids for improved computational efficiency in spectral element earth system models. *J. Adv. Model Earth Sy.*, 13(7):e2020MS002419, 2021.

[2] A. R. Herrington, P. H. Lauritzen, K. A. Reed, S. Goldhaber, and B. E. Eaton. Exploring a lower resolution physics grid in CAM-SE-CSLAM. *J. Adv. Model Earth Sy.*, page 2019MS001684, 5 2019.

[3] P. H. Lauritzen, P. A. Ullrich, C. Jablonowski, P. A. Bosler, D. Calhoun, A. J. Conley, T. Enomoto, L. Dong, S. Dubey, O. Guba, et al. A standard test case suite for two-dimensional linear transport on the sphere: results from a collection of state-of-the-art schemes. *Geosci. Model Dev.*, 7(1):105–145, 2014.

[4] J. Pudykiewicz, R Benoit, and A. Staniforth. Preliminary results from a partial LRTAP model based on an existing meteorological forecast model. *Atmosphere-ocean*, 23(3):267–303, 1985.

[5] Piotr K. Smolarkiewicz and Janusz A. Pudykiewicz. A class of semi-Lagrangian approximations for fluids. *Journal of Atmospheric Sciences*, 49(22):2082–2096, 1992.

[6] Paul A. Ullrich and Matthew R. Norman. The flux-form semi-Lagrangian spectral element (FF-SLSE) method for tracer transport. *Quarterly Journal of the Royal Meteorological Society*, 140(680):1069–1085, 2014.